

## Time Dependent Screening in the Photoionization of Doubly Excited Two-Electron Systems

C. Rosen,<sup>1</sup> M. Dörr,<sup>1,2,3</sup> U. Eichmann,<sup>1</sup> and W. Sandner<sup>1,2</sup>

<sup>1</sup>Max Born Institut, D-12489 Berlin, Germany

<sup>2</sup>Technische Universität, FB IV, D-10623 Berlin, Germany

<sup>3</sup>Université Libre, B-1050 Bruxelles, Belgium

(Received 7 June 1999)

We have investigated the two-electron dynamics of asymmetric doubly highly excited high angular momentum states in Sr interacting with a laser field. Even down to modest laser intensities the dominant fragmentation process is the photoionization of the inner electron. Analysis of the final ionic state reveals that the near-threshold ionization process is compatible with a time dependent screening of the nuclear charge on a time scale comparable to the orbit time of the outer electron. This is evidence of long-range dipolar correlation forces during the ionization process.

PACS numbers: 32.80.Fb, 31.70.Hq, 32.80.Rm

In the classic photoelectric effect the excess energy  $E$  of the photoelectron is related to the photon energy  $h\nu$  and the binding energy  $E_b$  through the formula  $E = h\nu - E_b$ . Deviations from this simple formula occur at high light intensities when the light-matter interaction is nonlinear, giving rise to the absorption of additional photons by the photoelectron in the continuum (above threshold ionization [1]). On the other hand, even at low light intensities, the photoelectron may exchange energy with the remaining multielectron ionic fragment, leaving the binding energy not uniquely defined. Examples of such multielectronic interaction are single-photon ionization with core excitation, single-photon double ionization [2], and inner shell photoionization followed by Auger decay [3]. These processes lead to complicated photoelectron energy distributions, depending on the detailed atomic structure. Finally, both nonlinear light matter interaction and electron correlation effects are present in the simultaneous multiple ionization of atoms in strong laser fields [4], a process whose explanation is still under active investigation. In all of these cases, the central question is: how does the core relax? Typically, for photoionization of ground state atoms, the relaxation of the remaining core proceeds diabatically, i.e., with a rapid removal of the photoelectron. This leads to the application of perturbation methods (“sudden approximation”) for the calculation of the final state distribution [5].

In the photoionization of excited atoms the same considerations apply. In the first experiments [6–9], Rydberg states of Ba were prepared and exposed to intense ps or fs laser pulses. Ionization of the *inner* valence electron is observed if the laser pulse duration is short compared to the round-trip time of the outer electron. Assuming an instantaneous removal of the inner electron, i.e., that the core charge seen by the outer electron changes suddenly from  $Z = 1$  to  $Z = 2$ , the final ionic state distribution of the remaining electron can be reproduced by a “shake” model, projecting the initial wave function of the outer Rydberg electron onto final ionic states.

In this Letter we present the first evidence of nonadiabatic phenomena in the photoionization of two electron systems. We investigate single ionization of doubly excited alkaline earth atoms by a laser photon. The results allow insights into both the relaxation in time of the remaining ion and the correlated electron dynamics, i.e., the energy exchange between the remaining bound Rydberg electron and the escaping photoelectron. These investigations are made possible by the observation that for special doubly excited states with both electrons in high  $\ell$  states the autoionization rate is very small. Therefore the laser-induced one-photon photoionization rate of the inner electron becomes dominant at laser intensities at about  $10^6$  W/cm<sup>2</sup>. This is almost 5 orders of magnitude lower than, e.g., in the experiment of Stapelfeld *et al.* [6]. At such low laser intensities, photoionization of the outer Rydberg electron is negligible. Our main result comes from the observation of the characteristic distribution of the final ionic Rydberg states. This distribution reveals a time dependent screening of the core charge for the remaining electron. It arises from the fact that the excess energy of the escaping electron is only slightly above the threshold. Thus there is enough time during the ionization process to allow for energy and angular momentum exchange between the outgoing electron and the remaining, highly excited ion. This leads to a strong polarization of the remaining ionic charge density distribution, which gives rise to dipolar (non-Coulombic) interaction in the continuum. Effects of such a long-range dipolar interelectronic interaction have previously been observed in the internal structure of bound two-electron systems [10,11]; they are found here also in the fragmentation process, i.e., in systems in which an electron is escaping. We will show that a time dependent picture is needed to describe quantitatively the observed final ionic state distributions.

Doubly excited states close to the double ionization continuum are ideally suited to observe correlated two-electron dynamics in external laser fields. In Ref. [12], e.g., Cohen *et al.* reported first evidence of a direct

one-photon double ionization of planetary states. Here, we investigate doubly excited Rydberg states in the vicinity of the  $N = 5$  threshold of  $\text{Sr}^+$ , approximately 2 eV below the double ionization continuum. The preparation of these states follows the well-established sequential resonant multiphoton excitation scheme [10,13].

The strontium atoms are first excited with two excimer laser pumped dye lasers from the  $\text{Sr}(5s^2)$  ground state via an intermediate resonance to a  $\text{Sr}(5sn_2\ell_2)$  Rydberg state in the presence of a ‘‘Stark switching’’ field, which allows one to select a high angular momentum  $\ell_2$  for the first (outer) electron [14]. About 1.5  $\mu\text{s}$  after the excitation of the first (outer) electron (giving enough time for adiabatic switch-off of the Stark field to zero), three more dye lasers, pumped by a second excimer laser, intersect the  $\text{Sr}^*$  beam. Lasers three and four excite the second (inner) valence electron via the  $5p_{3/2}n_2\ell_2$  to the  $5d_{5/2}n_2\ell_2$  resonances. The strongest fifth laser (1 mJ pulse energy, much larger than the approximately 10  $\mu\text{J}$  pulse energy of the first four lasers) excites the atom further to the  $5fn\ell/5gn'\ell'$  series. Thus, the fifth laser is used both to prepare the autoionizing state and to photoionize it. Approximately 200 ns after the fifth laser, a detection field pulse (20 ns rise time, up to 12 kV/cm) is applied to the interaction region. Depending on its amplitude, it may field ionize the ionic Rydberg states to  $\text{Sr}^{2+}$ , and it pushes them towards a time-of-flight detector.

Figure 1(a) shows an absorption spectrum taken in the vicinity of the  $N = 5$  ionic threshold, starting from the  $5d_{5/2}n_2 = 16, \ell_2 = 10$  state, at a high detection field strength. The  $\text{Sr}^{2+}$  yield as a function of the photon energy of the fifth laser is shown. Above the  $\text{Sr}^+$   $5f$  threshold, indicated by the vertical dashed line, the unperturbed  $5gn'\ell'$  series with  $n' > 19$  is visible. Below the  $\text{Sr}^+$   $5f$  threshold, resonances of both the  $5fn\ell$  and the  $5gn'\ell'$  series are excited. Figure 1(b) shows the same spectrum at a detection field strength of 0.2 kV/cm. The figure clearly shows that the detection of the resonances below the  $\text{Sr}^+$   $5f$  threshold strongly depends on the

applied field strength, whereas the signal for resonances above this threshold is unchanged.

To explain this behavior we must compare the rates for autoionization and for photoionization by the fifth laser.

(i) If the doubly excited atom autoionizes, the ion is left in a low excited state which cannot be efficiently photoionized with the present lasers or field ionized with accessible detection field strength. This holds for initial states below the  $\text{Sr}^+$   $5f$  threshold. For the  $5gn'\ell'$  resonances above the  $\text{Sr}^+$   $5f$  limit, however, the autoionization process leaves the ion to a large amount in the  $\text{Sr}^+$   $5f$  state which can be photoionized with a single photon to yield  $\text{Sr}^{2+}$ . This process therefore dominates for the  $5gn'\ell'$  resonances above the  $\text{Sr}^+$   $5f$  threshold.

(ii) If the doubly excited atom absorbs a photon before autoionization takes place, most likely the inner electron photoionizes, while the outer electron remains in a highly excited Rydberg state. In contrast to similar experiments [8,12], the inner electron in our case is photoionized by a *single* photon since it is already in an excited state. Since the autoionization rate scales with the principal quantum number as  $n^{-3}$ , preferentially the higher Rydberg states of the  $5fn\ell$  series are sufficiently long lived to absorb an additional photon. This photoionization process can be unambiguously detected for resonances below the  $\text{Sr}^+$   $5f$  continuum by field ionizing the remaining ionic state. The competing autoionization process, discussed in the previous paragraph, leads to more deeply bound singly charged states, which are not detected in our experiment.

Now, the question we address is to what extent the two electrons exchange energy and angular momentum during the photoionization process of the inner electron. By analyzing the final ionic state distribution, for a well-defined initial Rydberg state, we obtain a sensitive quantitative probe of the energy exchange.

We tune the laser to a particular  $5fn\ell$  resonance with  $25 < n < 48$  and measure the  $\text{Sr}^{2+}$  yield as a function of the detection field pulse strength. We use the classical field ionization formula  $F = Z^3/16N^4$  (in a.u.), where  $Z = 2$  is the charge of the  $\text{Sr}^{2+}$  core, to deduce the principal quantum number  $N$  of the final ionic Rydberg state from the detection field strength  $F$  [15].

Figure 2 shows the final ionic state distributions for three different initial states  $5fn\ell$ . As a first attempt to interpret the data we recall the diabatic model. The probability  $|c_{N\ell}|^2$  of finding the ion in a specific  $N\ell$  state is given by the square of the overlap integral  $|\langle n\ell | N\ell \rangle|^2$  of the initial and final wave function for the residual valence electron [16]. The maximum probability is obtained for those initial and final wave functions having similar radial expectation values. This is fulfilled for the final ionic principal quantum number  $N = \sqrt{2}n$ . In our experiment, the ionic signal is composed of all ionic Rydberg states field ionized down to a lower limit for  $N$  given by the field strength of our detection field pulse. To compare with theory we have to sum up all

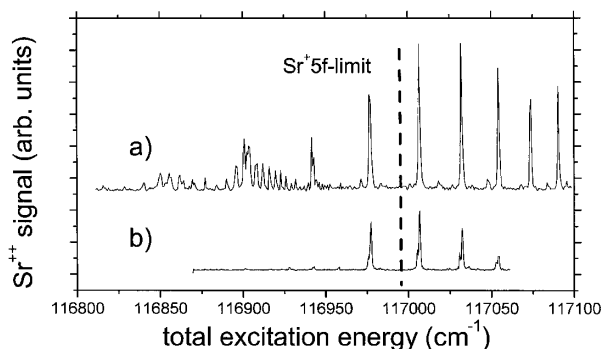


FIG. 1. Absorption spectra of planetary resonances, excited from the  $5d_{5/2}n_2 = 18, \ell_2 = 10$  double Rydberg state. The detection field strength is (a) 12 kV/cm and (b) 0.2 kV/cm.

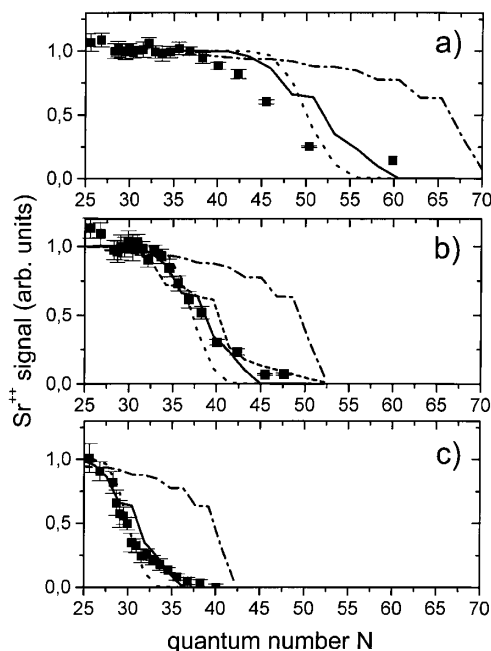


FIG. 2. Final ionic state distribution after photoionization of the  $5fn\ell$  resonances with (a)  $n = 48$ , (b)  $n = 36$ , and (c)  $n = 28$ . The dashed-dotted curves give the theoretical adiabatic results, the solid curves give the theoretical adiabatic results for  $t_f = t_n = 2\pi n^3$ , the dotted curve is  $t_f = 2t_n$ , and the solid squares with the error bars give the experimental data. In (b) additional theoretical data for  $t_f = 0.6t_n$  are shown (short dashed curve).

allowed contributions

$$S(N) = \sum_{N'=N}^{\infty} |\langle n\ell | N'\ell \rangle|^2 \quad (1)$$

to obtain the ion yield signal. The results are displayed in Fig. 2 (dashed-dotted curves). We see that they are clearly not in accord with the experimental data points. The adiabatic theoretical curves predict distributions centered around a too high  $N$ , and the shape of the threshold does not reflect the experimentally measured distribution, indicating the breakdown of the adiabatic approximation.

In order to explain the final ionic state distribution observed, we solve a time dependent radial Schrödinger equation [17] for the outer electron. We model the energy exchange by a time dependent effective core charge  $Z = Z(t)$  seen by the outer electron. We change  $Z(t)$  linearly from 1 to 2 between  $t = 0$  and  $t = t_f$ . In the figures, we give the switch time  $t_f$  in units of the classical orbital period of the electron in the initial Rydberg state  $t_n = 2\pi n^3$  a.u. We do not consider the feedback of the outer electron on the escaping photoelectron. Our initial state is a Rydberg eigenstate with quantum numbers  $n$  and  $\ell$  for the outer electron with  $Z = 1$ , as it is prepared in the experiment. We solve the Schrödinger equation for different  $t_f$  and obtain the coefficients of the final ionic ( $Z = 2$ ) state distribution by projecting the calculated final wave packet onto the ionic eigenstates.

An example of the final radial wave function and the ionic state distribution, for  $t_f = t_n = 3 \times 10^5$  a.u., is shown in Figs. 3(b) and 3(c). The initial wave function, chosen as  $n = 36$ ,  $\ell = 0$ , is shown in Fig. 3(a). The results can be safely scaled between the large Rydberg quantum numbers, as shown by the results for  $n = 20$ , superposed in Fig. 3(c): The envelope of the probability distribution is unchanged. Summing over the distribution shown in Fig. 3(c) as in Eq. (1), the results of the calculation can be directly compared to the experimental data. Figure 2 shows that excellent agreement is achieved when we assume the core charge to change on a time scale of the orbital period of the outer electron. The ratio  $N/n$  is roughly 1 for the most likely final ionic  $N$  state, indicating that the remaining electron is more tightly bound than expected from the diabatic shake model [18].

Since the final ionic state distribution reflects directly the energy transferred to the escaping electron, we can alternately analyze our results in terms of an energy budget for the electrons. Let us first consider a classical isotropic ( $s$ -wave) model, where the charge of the electron is located on a spherical surface at a given radius. The potential for the escaping electron with radial coordinate  $r_1$  is

$$V(r_1) = \begin{cases} -2/r_1 & \text{for } r_1 < r_0, \\ -1/r_1 & \text{for } r_1 > r_0, \end{cases} \quad (2)$$

while the outer electron is fixed at a given  $r_0$ . Solving the classical equation of motion for the inner electron, we obtain the energy transferred from the remaining electron (at  $r = r_0$ ) to the photoelectron. We note that in this case the screening changes completely diabatically. In the calculation the inner electron starts at  $r_1 = 25$  a.u., the

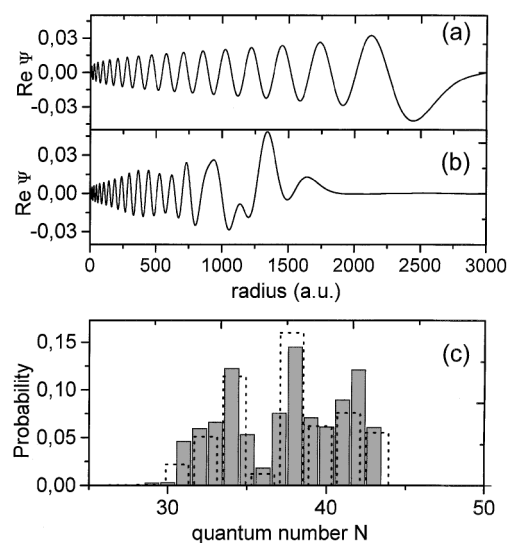


FIG. 3. (a) Initial  $n = 36$  wave function. (b) Real part of the final ionic wave packet. (c) Final ionic state probability distribution from the projection of the final wave packet onto the ionic Rydberg eigenstates. Dashed boxes: results for  $n = 20$ , scaled to  $n = 36$ .

outer classical turning point of the  $\text{Sr}^+ 5f$  state, with an initial velocity  $v_i$  of about 0.40 a.u. as given by the experimental condition  $E = v_i^2/2m = E_b + h\nu + V(r_1)$ , where  $E_b$  is the binding energy of the inner electron (ignoring the outer electron) and  $h\nu$  is the photon energy of the ionizing laser. The energy transfer to the photoelectron, at the expense of an increased binding energy of the remaining ionic Rydberg electron, can be expressed in terms of the ratio  $N/n$ , which can be compared to the experimental results. For  $r_0 = 1.5n^2$ , which is the radial expectation value for low  $\ell$  states, we find the ratio  $N/n = 1.32$ , while for  $r_0 = 2n^2$ , the classical outer turning point, we find  $N/n = 1.42$ , corresponding to the most likely energy transfer associated with the shake model. However, in the experiment, as discussed above, we find the adiabatic ratio  $N/n = 1$ . As a first step beyond the isotropic  $s$ -wave model we add a dipole interaction term  $r_0 \cos(\vartheta)/r_1^2$  to the potential  $V(r_1)$  for  $r_1 > r_0$ , where  $\vartheta$  is the angle between the position vectors of the two electrons. We obtain  $N/n = 1$  if we set  $\vartheta = 0$  in the dipole term and neglect any further angular dependence. This result implies that the angular interaction is necessary to explain the experimental observations. The escaping electron polarizes the remaining electron-ion subsystem forming an extreme Stark state. The resulting dipole is oriented with both electrons on the *same* side of the nucleus to account for the large energy transfer. Such configurations are known to exist as a special class of doubly excited states [19].

We note that the time it takes for the inner electron to pass the outer at its radial expectation value, based on a classical calculation, is a factor of 10 shorter than the orbital period of the outer electron. However, the critical radius  $r_c$ , beyond which the long-range correlations can no longer mix the ionic  $N$  states, is given by  $r_c = \sqrt{3N^5/8}$  [20]. This increases the effective interaction time up to a factor of 5, thus restoring the adiabatic nature of the ionization process. Thus, the adiabatic screening is the result of a long-range correlation acting during the escape of the ionizing inner electron.

In summary, we have analyzed the fragmentation dynamics of doubly excited states in a weak laser field. Direct autoionization decay is strongly reduced over a wide range of initial states and therefore, even at modest laser intensities, the dominant process is the photoionization of the “inner” electron, followed by a readjustment of the outer electron in highly excited ionic states. We have obtained the ionic final state distribution from field ionization. The high density of Rydberg states allows a detailed analysis of the energy redistribution due to the interelectronic interaction between the outgoing photoelectron and the highly polarizable wave function of the remaining Rydberg electron during the ionization process. The process can be quan-

titatively explained with a time dependent model, where the energy exchange between the electrons is reduced to a time dependent effective core charge experienced by the remaining electron. This provides evidence for long-range time dependent correlation forces during the ionization process which may be explained through a mechanism similar to “postcollision interaction” [21,22], but with the additional inclusion of long-range dipolar interactions (angular momentum exchange) in the continuum.

We thank M. Seng for his technical assistance during the early stage of this work. We acknowledge financial support from the Deutsche Forschungsgemeinschaft.

- 
- [1] P. Agostini *et al.*, Phys. Rev. Lett. **42**, 1127 (1979).
  - [2] R. Wehlitz *et al.*, Phys. Rev. Lett. **67**, 3764 (1991).
  - [3] V. Schmidt, *Electron Spectrometry of Atoms using Synchrotron Radiation* (Cambridge University Press, Cambridge, England, 1997).
  - [4] B. Walker *et al.*, Phys. Rev. Lett. **73**, 1227 (1994).
  - [5] L.D. Landau and E.M. Lifshitz, *Quantum Mechanics* (Pergamon Press, Oxford, 1977).
  - [6] H. Stapelfeldt *et al.*, Phys. Rev. Lett. **67**, 3223 (1991).
  - [7] R.R. Jones and P.H. Bucksbaum, Phys. Rev. Lett. **67**, 3215 (1991).
  - [8] R.B. Vrijen and L.D. Noordam, J. Opt. Soc. Am. B **13**, 189 (1996).
  - [9] D.A. Tate and T.F. Gallagher, Phys. Rev. A **58**, 3058 (1998).
  - [10] U. Eichmann, V. Lange, and W. Sandner, Phys. Rev. Lett. **64**, 274 (1990); **68**, 21 (1992).
  - [11] P. Camus and S. Cohen, Phys. Rev. A **51**, 1985 (1995); Phys. Rev. A **52**, 2486(E) (1995).
  - [12] S. Cohen, P. Camus, and A. Bolvinos, J. Phys. B **26**, 3783 (1993).
  - [13] M. Seng *et al.*, Phys. Rev. Lett. **74**, 3344 (1995).
  - [14] R.R. Freeman and D. Kleppner, Phys. Rev. A **14**, 1614 (1976).
  - [15] We checked the validity of the field ionization formula for ions separately by exciting  $\text{Sr}^+ \text{Ng}$  states ( $20 < N < 65$ ; magnetic quantum number  $|m| \leq 4$ ) and measuring their field ionization thresholds. States with  $|m| > 4$  are not populated in the experiment.
  - [16] N.H. Tran, R. Kachru, and T.F. Gallagher, Phys. Rev. A **26**, 3016 (1982).
  - [17] See, e.g., W.H. Press *et al.*, *Numerical Recipes* (Cambridge University Press, Cambridge, England, 1992), p. 842.
  - [18] A different approach has been pursued by W. Huang, U. Eichmann, and W. Sandner [Phys. Rev. A **59**, 2744 (1999)].
  - [19] K. Richter and D. Wintgen, J. Phys. B **24**, L565 (1991).
  - [20] P. Camus *et al.*, Phys. Rev. Lett. **62**, 2365 (1989).
  - [21] A. Niehaus, J. Phys. B **10**, 1845 (1977).
  - [22] P. van der Straten *et al.*, Z. Phys. D **8**, 35 (1988).